Optimizing Chain Bridging in Complex Block Copolymers

François Drolet† and Glenn H. Fredrickson*

Department of Chemical Engineering and Materials Research Laboratory, University of California, Santa Barbara, California 93106

Received January 16, 2001; Revised Manuscript Received May 7, 2001

ABSTRACT: Recent experiments by Ryu, Hermel, and co-workers have demonstrated a correlation between the presence of bridging A-blocks and practical toughness in themoplastic ABABA pentablock copolymers. Building on this observation, we develop a computational tool for evaluating average bridging fractions of internal blocks in complex block copolymers and apply the tool to the optimization of bridging fractions in mesophase structures computed with self-consistent-field theory. We identify optimal molecular designs for ABABA pentablock copolymers that could provide the useful combination of high modulus and high toughness. Further applications of the approach to property screening in complex mesophases formed by ABC and ABCA block copolymers are discussed.

1. Introduction

Our understanding of the thermodynamic principles that dictate self-assembly in block copolymers has advanced dramatically over the past several decades. It is now possible to carry out a "first principles" design of a variety of simple block systems with AB diblock, ABA triblock, or $(AB)_n$ starblock architectures to produce lamellar, hexagonal, bcc spherical, and even exotic "gyroid" bicontinuous mesophases.[1,2] Theory has played an important role in this development, not only by providing a unifying framework in which to organize experimental observations but also by identifying and rationalizing a variety of metastable structures found in experiment.[3] The implementation of polymer self-consistent-field theory (SCFT) due to Matsen and Schick[4,5] has been particularly influential because it allows for structural and thermodynamic analysis of spatially periodic mesophases with arbitrarily complex symmetry, such as the $Ia\bar{3}d$ space group of the gyroid phase.

Armed with this increased understanding of self-assembly principles and improved synthetic methods, experimentalists have in recent years launched investigations of block copolymer systems of increasing architectural complexity and increasing numbers of chemically distinct blocks. For example, flexible copolymers with either linear ABC or star ABC architectures have been prepared and investigated by a number of groups.[6−10] These studies have shown that as the number of distinct blocks is increased from two to three, there is a dramatic increase in both the complexity and variety of self-assembled structures. This richness of self-assembly behavior can be traced to the "frustration" associated with an inability to satisfy an increased number of binary interactions (quantified by interfacial tensions or Flory "χ" parameters). In particular, the preferred contacts between dissimilar blocks often prove inconsistent with the block connectivity provided by a particular copolymer architecture. This frustration leads to fascinating structures such as the "knitting pattern"[6] and the core−shell gyroid mesophases.[7−9] Although not a focus of the present paper, we note that even richer self-assembly behavior is possible in block copolymer systems with rigid or otherwise sterically constrained blocks (e.g., liquid crystalline, dendrimer, or conjugated blocks).

A difficulty in carrying out systematic morphological studies of such "complex" block copolymers is that the experimental parameter space (e.g., block compositions, molecular weights, architecture, temperature) is very large and therefore laborious to explore. Moreover, chemistries capable of producing well-controlled block structures do not often lend themselves to massively parallel synthesis and morphological characterization is often problematic. Thus, theory will likely prove even more important in guiding experimentation as the focus moves to ever more complex block copolymer systems.

A disadvantage of the Matsen−Schick implementation of SCFT for the purpose of identifying new types of mesophases and mapping out phase diagrams in complex block copolymer systems is that it requires a *symmetry assumption* prior to optimization of the structure of a phase and free energy evaluation. This can evidently be a limitation in an experimentally unexplored system with many competing interactions, where little intuition exists about the optimal spatial arrangement of dissimilar block segments. We recently developed a new real-space implementation of SCFT that should prove useful in this regard.[11] Unlike the Matsen−Schick approach, we attempt to identify mesophases by an optimization procedure in which the only symmetry condition is imposed by overall periodic boundary conditions on a simulation cell. Starting from a randomly selected, disordered initial condition, the set of chemical potential fields is adjusted to lower the free energy of the system, subject to the constraint of incompressibility and enforcing required self-consistency relations between the chemical potentials and their conjugate monomer density fields. The algorithm effectively performs a quench on the free energy landscape to structures corresponding to local and/or global minima. Because quenches using different random initial conditions (or for different parameter values) are statistically independent, quenches can be performed in parallel—permitting a "computational−combinatorial screening" for novel types of self-assembly.

† Present address: Hyperdigm Research, 102 De Gascogne, St-Lambert, Qc., J4S-1C8.

10.1021/ma0100753 CCC: $20.00
Published on Web 06/19/2001

A recent application of the above procedure to a "complex" model system, linear ABCA tetrablock copolymers, unearthed several new mesophases.[11] We note that a similar computational approach has recently been reported by Bohbot-Raviv and Wang,[12] which is based on an approximate density functional theory, rather than the full SCFT. The Fraaije group has also been quite active in the related area of dynamic density functional theory of polymers, although their method has been primarily applied to simple, rather than complex, block copolymers to date.[13] Very recently, Dotera et al.[14] applied lattice Monte Carlo simulation methods to investigate the self-assembly of ABC and ABCD starblock copolymers. This method is complementary to the SCFT approach followed here, although more computationally demanding.

In the design of block copolymers for applications, one generally aims to optimize a set of *physical properties* rather than to achieve a particular type of self-assembly. Thus, if the computational−combinatorial strategy outlined above is to have maximum impact, the structures that are unearthed by the SCFT code should be further examined by a software tool, a "property engine", to associate one or more physical properties (e.g., modulus, dielectric constant, birefringence, thermal conductivity, etc.) with each structure. A third piece of software, an "optimizer", could then be used to interface with the SCFT code and the property engine in order to identify molecular designs of copolymers that provide optimal combinations of properties.

Unfortunately, the morphology−property link remains weak in a number of key areas. Property engines built around continuum composite media packages that associate effective *linear* elastic moduli with block copolymer mesophases are straightforward to envision. Schemes to approximately compute dielectric or optical properties, such as birefringence or dichroism, for the various mesophases could also be devised. More difficult is the assignment of nonlinear elastic properties and *practical toughness* to a candidate mesophase structure.

Recent experiments on a series of hydrogenated diblock, triblock, and pentablock copolymers have demonstrated that, at least within this class of materials, practical toughness can be roughly correlated with the fraction of inner blocks that bridge (rather than loop) across domains.[15,16] More specifically, a series of microphase-separated block copolymers based on poly(vinylcyclohexane) (PCHE)[17] and polyethylene (PE) were examined mechanically in both thin film deformation studies[15] and microtensile experiments.[16] Because of the large difference in entanglement molecular weight between PE and PCHE and the modest molecular weights employed (<100 000), the PE domains in these materials consist of well-entangled PE blocks, while the PCHE domains are filled with PCHE blocks that are virtually unentangled. PCHE−PE diblocks are extremely brittle across the entire composition range. Glass-rich (70% PCHE, symmetric end blocks) PCHE−PE−PCHE triblocks were found to be tougher than homopolymer PCHE but still exhibit brittle failure via crazing. In contrast, glass-rich (70% PCHE) PCHE−PE−PCHE−PE−PCHE pentablocks of comparable overall molecular weight exhibited a dramatic increase in toughness, exhibiting ductile failure via shear transformation zones.[15] This increase in toughness is believed to arise from the presence of "bridging" PCHE blocks in the pentablock materials. As illustrated in Figure 1,

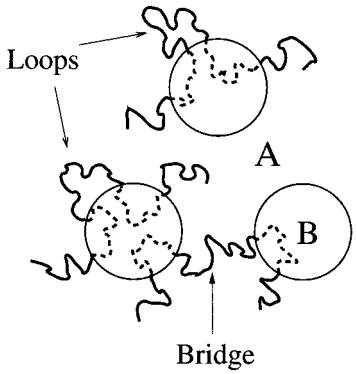

Figure 1. Bridging and looping in A-rich ABABA pentablock copolymers. The center A blocks (glassy) provide some concentration of bridging "tie chains" across the continuous A domains that separate the discrete (rubbery) B domains. Upon strong deformation, fracture in the A continuous phase must be preceded by cleavage of the tie chains or pull-out of the BA diblock ends. Either process likely contributes to the observed toughness of such materials.

for such an architecture the *center* PCHE blocks have the option of having their terminal ends at the interfaces of two different PE aggregates (bridges) or at two different points on the interface of a single PE aggregate (loops). Bridges obviously present significant resistance to fracture since in order to propagate a crack, the bridging blocks must either be cleaved or have a PE−PCHE dangling end pulled out of the mesophase (leading to a great deal of energy dissipation). Recent experiments by Ryu[18] have systematically varied bridge fraction by diluting pentablocks with triblocks and confirmed the significance of bridging conformations for thin film strength.

The aforementioned experiments clearly establish a link between the existence of bridging central PCHE blocks in the pentablock copolymers and toughness. Nevertheless, it is important to note that many other factors can influence the practical toughness of such materials, including grain size and orientation of the mesophase morphology, processing and thermal history, molecular weight, etc.[19] While acknowledging these factors, it is useful for the present purposes of constructing a simple "toughness property engine" to associate improved practical toughness with higher bridging fractions. Such information on average bridge fraction is readily accessible in a SCFT calculation, as has been described by Matsen and Schick.[20−22] Once the converged self-consistent potential fields have been determined for a given system, either by the Matsen−Schick spectral method or by the real-space algorithm described in the next section, the SCFT diffusion equation need only be solved one additional time within a single unit cell of a periodic mesophase in order to compute the bridge fraction of a targeted internal block.

In the present paper, we discuss the implementation of such a property engine that is well-suited for toughness screening in tandem with our real-space SCFT code. Because our code (running in a "discovery" mode) returns structures that contain more than one unit cell of a given mesophase, we depart slightly from the single-cell approach of Matsen and Schick. Given a computed equilibrium structure, we first construct a Voronoi diagram around a particular discrete phase (e.g., the hexagonally packed PE cylinders of a pentablock mesophase) to identify the primitive cells composing the structure. Next, we solve the diffusion equation in the

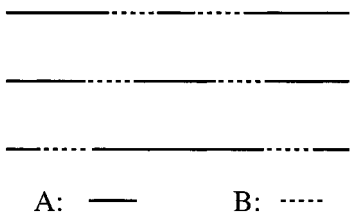

Figure 2. Examples of the symmetric ABABA pentablocks that are considered in the present study. The middle A block volume fraction f_3 is increased from top to bottom, while holding the total volume fraction of the (hard) A blocks fixed at $f_A = f_1 + f_3 + f_5 = 0.7$. With the additional conditions of symmetry, $f_1 = f_5$ and $f_2 = f_4$, there is only a single composition degree of freedom, which we choose to be f_3. Increasing f_3 can be viewed as sliding the two fixed-composition B blocks symmetrically away from the center of a molecule.

computed mean fields to analyze the conformational statistics of any desired internal block throughout the structure. By integrating the two-point statistical information within each primitive cell, a bridge fraction can be associated with each cell. These bridge fractions are then averaged over all cells to compute an average bridge fraction for the overall structure.

The outline of the present paper is as follows. In section II, we review the basic equations of SCFT and briefly summarize the method used to equilibrate mesophase structures. We then describe our implementation of the bridge fraction-based "property engine" that was sketched above. In section III, we apply the method to analyze bridge fractions in a pentablock system similar to the PCHE−PE−PCHE−PE−PCHE pentablocks considered by Ryu et al.[15] In particular, we consider ABABA pentablocks that are symmetric about their midpoint; i.e., the outer A (glassy) blocks are fixed to be equal length (equal volume fractions $f_1 = f_5$), and the inner B (rubbery) blocks are also constrained to be the same size ($f_2 = f_4$). Since generally one desires to maximize toughness at fixed modulus, we consider varying the middle block composition, f_3, subject to fixed overall glass content, i.e., $f_A = f_1 + f_3 + f_5$ fixed. This variation in architecture can be viewed as a symmetric "sliding" of the B blocks along the chain contour, as illustrated in Figure 2. Our results suggest that the center A block bridge fraction can be maximized by a particular choice of f_3 (approximately 0.5 for $f_A = 0.7$), the implication being that symmetric pentablock copolymers with 70% glass content might be optimally tough when they possess a 5 to 1 ratio of center A block length to end A block length. In section IV, we provide a few examples of applying the method to calculating bridge fractions for some novel complex mesophases that were recently identified with our SCFT screening tool. Finally, in section V, we summarize our results and discuss further applications and extensions.

2. Theory

In this section, we outline the formulation of self-consistent-field theory (SCFT) for a melt of ABABA pentablock copolymer chains with polymerization index N. We adopt the notation of Matsen and Schick[4] and refer the reader there for additional details. Within SCFT, a mean-field theory, one considers the statistics of a single copolymer chain in a set of effective chemical potential fields ω_K. These potential fields, which replace the actual interactions between different chains in the melt, are conjugate to the monomer density fields ϕ_K, of block species K. (We invoke an incompressible model and normalize densities so that the ϕ_K fields can be interpreted as local volume fractions of monomer species K.) For such an ABABA melt, the free energy per chain (in units of k_BT) is given by

$$F = -\ln(Q/V) + \frac{1}{V}\int d\mathbf{r}\,[\chi_{AB}N\phi_A\phi_B - \omega_A\phi_A - \omega_B\phi_B - P(1 - \phi_A - \phi_B)] \quad (1)$$

where χ_{AB} is the usual Flory−Huggins parameter describing the strength of A−B monomer interactions, V is the volume of the system, $P(\mathbf{r})$ is a Lagrange multiplier (a "pressure") that is chosen to enforce incompressibility, and $Q = \int d\mathbf{r}\; q(\mathbf{r},1)$ is the partition function of a single chain in the effective fields ω_A and ω_B. The end-segment distribution function $q(\mathbf{r},s)$ gives the probability that a section of a chain, of contour length s and containing a free chain end, has its "connected end" located at $\mathbf{r}$. The parametrization is chosen such that the contour variable s increases continuously from 0 to 1 from one end of the chain to the other. With the use of a flexible Gaussian chain model to describe the single-chain statistics, the function $q(\mathbf{r},s)$ satisfies a modified diffusion equation

$$\frac{\partial q}{\partial s} = \nabla^2 q - [\theta_1(s) + \theta_3(s) + \theta_5(s)]\omega_A(\mathbf{r})q - [\theta_2(s) + \theta_4(s)]\omega_B(\mathbf{r})q \quad (2)$$

where

$$\theta_i(s) = \begin{cases} 1, \text{ if s belongs to block } i \\ 0, \text{ otherwise} \end{cases} \quad (3)$$

In eq 2, lengths were scaled by the (overall) radius of gyration of an unperturbed chain. The appropriate initial condition is $q(\mathbf{r},0) = 1$. Unless the pentablock chain is symmetric (i.e., $f_1 = f_5$ and $f_2 = f_4$, where f_i is the volume fraction of block i), the two ends are distinct, so that a second distribution function $q^\dagger(\mathbf{r},s)$ describing the conjugate piece of chain (containing the other chain end) is needed. This function satisfies the initial condition $q^\dagger(\mathbf{r},1) = 1$ and obeys eq 2 with $q^\dagger$ in place of q and with a minus sign on the right-hand side. Expressed in terms of q and $q^\dagger$, the total density of A monomers is

$$\phi_A(\mathbf{r}) \equiv \sum_{i=1,3,5} \phi_A^i(\mathbf{r}) = (V/Q) \sum_{i=1,3,5} \int_0^1 ds\; q(\mathbf{r},s)\, q^\dagger(\mathbf{r},s)\, \theta_i(s) \quad (4)$$

where ϕ_A^i is the contribution to the density coming from block i. We note that this expression can be derived by requiring that F be minimized with respect to variations in the potential field ω_A. A similar expression holds for $\phi_B(\mathbf{r})$ but is summed over blocks 2 and 4. Minimization of F with respect to ϕ_A, ϕ_B, and P leads to the three equations

$$\omega_A(\mathbf{r}) = h(\phi_B(\mathbf{r}) - f_B) + P(\mathbf{r}) \quad (5)$$

$$\omega_B(\mathbf{r}) = h(\phi_A(\mathbf{r}) - f_A) + P(\mathbf{r}) \quad (6)$$

$$\phi_A(\mathbf{r}) + \phi_B(\mathbf{r}) = 1 \quad (7)$$

which complete the theory. In the above, $f_A = f_1 + f_3 + f_5$ and $f_B = f_2 + f_4$. We have also introduced the

shorthand $h \equiv \chi_{AB}N$ for the A−B block interaction strength and imposed constant shifts in the potential fields ω_A and ω_B. SCFT has been applied to a number of model block copolymer melts and solutions, as well as to binary and ternary alloys of block copolymers with homopolymers, in both bulk and thin films.[5,23] The implementation of the theory first proposed by Matsen and Schick[4] has been especially successful at predicting phase behavior in these systems. In their approach, all spatially dependent fields in the SCF equations are expanded in a finite set of basis functions appropriate for an assumed mesophase symmetry. The amplitude of every term in the series for the effective fields is then adjusted (using, for instance, a Newton−Raphson method) until the SCF equations are satisfied. The calculation is repeated for all competing mesophases, and the one with lowest free energy is identified as the equilibrium structure.

In our implementation of the theory, we instead solve the SCF equations directly in real space, within a two-dimensional (or three-dimensional) rectangular (or cubic) simulation box with periodic boundary conditions. Our algorithm comprises six steps which are now described for the ABABA copolymer melt:

(1) Define a uniform grid within the simulation cell. Set the initial values of ω_A and ω_B at every point on the grid using a random number generator.

(2) Set the effective pressure field P to $P = {}^1/_2(\omega_A + \omega_B)$. This expression is obtained by adding eqs 5 and 6 and using the condition of incompressibility, eq 7. The average value of P is chosen to be zero.

(3) Solve the modified diffusion equations for q and $q^\dagger$ along the entire contour length of a chain using an alternating direction implicit method.

(4) Evaluate the monomer densities ϕ_A and ϕ_B conjugate to ω_A and ω_B using eq 4 and the corresponding equation for ϕ_B.

(5) Update the potential fields ω_K for K = A, B locally by using the prescription

$$\omega_K^{new} = \omega_K^{old} + \lambda \left(\frac{\delta F}{\delta \phi_K}\right)^*$$

where $(\delta F/\delta\phi_{A(B)})^* = h(\phi_{B(A)} - f_{B(A)}) + P(\mathbf{r}) - \omega_{A(B)}^{old}$.

(6) Return to step (2).

This iterative procedure continues until the free energy converges to a local minimum. The parameter λ appearing in step (5) determines how large a step is taken along the local gradient direction at each iteration. The results presented below for the pentablock melt were obtained using the value $\lambda = 0.1$. Larger values of λ can speed up convergence but also may lead to numerical instabilities. It should also be pointed out that our original implementation of SCFT in real space used a slightly different algorithm in which a linear mix of old and new solutions was used to update the volume fractions instead of the potential fields. That first algorithm, outlined in ref 11, identified several new forms of self-assembly in ABCA tetrablock melts, including the mesophases reproduced in Figures 10 and 11. It is not guaranteed that both algorithms converge to the same structures, especially for the more complex ABC and ABCA systems, where competing interactions may produce rough free energy landscapes with many metastable local minima. As with any nonlinear optimization problem, the quality of the results obtained (i.e., the lowest free energy structure unearthed) may vary widely among different algorithms and with modifications of the physical system. In the case of ABABA pentablock copolymer melts, we found that both algorithms produce the same morphologies. The newer implementation was selected because of its superior performance.

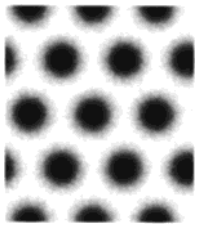

Figure 3. Total A density field $\phi_A(\mathbf{r})$ for a symmetric ABABA pentablock copolymer melt with block volume fractions $f_1 = f_5 = 0.09$, $f_2 = f_4 = 0.15$, $f_3 = 0.52$, and $h = \chi_{AB}N = 45$. This equilibrium hexagonal phase (B-rich cylinders are dark) was obtained with the algorithm of section II, employing a 70×81 rectangular lattice with grid size $\Delta x = 0.0975R_g$, where $R_g^2 = Nb^2/6$ is the unperturbed mean-squared radius-of-gyration of a copolymer.

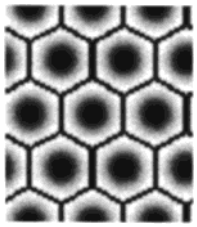

Figure 4. Voronoi diagram constructed from the hexagonal phase shown in Figure 3.

Next, we turn to discuss how SCFT can be used to examine the conformational statistics of specific blocks along a copolymer chain.[20−22] Here we consider a *symmetric* ABABA pentablock copolymer melt ($f_1 = f_5$, $f_2 = f_4$) in a region of the parameter space where B blocks self-assemble into cylinders dispersed in a matrix rich in A. Moreover, our focus is on the bridging vs looping behavior of the middle A block (block 3), since that has been correlated with practical toughness in experiments. To determine the fraction of middle A blocks that form bridges between neighboring B cylinders, we start from an "equilibrium" configuration for the fields ω_A and ω_B, obtained using the algorithm presented above. For computational efficiency, such calculations can be done in two dimensions, assuming homogeneity along the cylinder axes of the hexagonal mesophase.

A typical configuration is shown in Figure 3. It consists of a relatively large number of circular B domains (dark), each one with a coordination number of six. The first step in computing the midblock bridging fraction is to determine for each cylindrical domain the set of points on the lattice that lie closer to its center than to the center of any other cylindrical domain. The boundary enclosing such a domain is known as a Voronoi polygon, and it acts as a unit cell for the structure. The set of all Voronoi polygons defined in this manner forms a Voronoi diagram such as the one shown in Figure 4. Next, we focus on a single Voronoi cell D_1 and, following Matsen and Thompson,[22] define the function

$$\bar{q}(\mathbf{r}, f_1+f_2) = \begin{cases} q(\mathbf{r}, f_1 + f_2) & \text{if } r \text{ belongs to } D_1 \\ 0 & \text{otherwise} \end{cases} \quad (8)$$

which constrains the junction between the second and

third blocks of a pentablock chain to cell D_1. The diffusion equation for $\bar{q}$, eq 2 with $q \rightarrow \bar{q}$, is then solved forward in s, starting from this initial value at $s = f_1 + f_2$ up to $s = f_1 + f_2 + f_3$. The probability that the middle A block of a chain has both of its ends located in cell D_1 is finally given by

$$f_{\mathrm{lp}} = \frac{V}{V_{D_1} Q} \int_{D_1} \mathrm{d}\mathbf{r}\; \bar{q}(\mathbf{r}, f_1 + f_2 + f_3)\, q^{\dagger}(\mathbf{r}, 1 - f_1 - f_2 - f_3) \tag{9}$$

where V_{D_1} is the volume of cell D_1. f_{lp} thus represents the fraction of chains that have their middle A block in a looped configuration. The fraction of bridges is simply given by $f_{\mathrm{br}} = 1 - f_{\mathrm{lp}}$. An average value of f_{br} is obtained by repeating the calculation for all domains in the configuration and performing an arithmetic average.

While the above method of computing bridge fractions has been discussed in the context of the central block of ABABA pentablock copolymers, the approach is clearly much more general and, with suitable modifications, can be applied to internal blocks of any type of mesophase or copolymer architecture.

3. Application to Pentablock Copolymers

In the present section, we apply the formalism of the previous section to the problem of optimizing practical toughness in a class of symmetric ABABA pentablock copolymers. Here we imagine that at ambient temperature block component A is an amorphous "hard" block (e.g., PS, PMMA, or PCHE), while component B is a "soft" block (e.g., PB, PI, or PE). We further focus on thermoplastic applications where a *high modulus* is desired, so we restrict attention to materials with a 70% overall glass content ($f_A = f_1 + f_3 + f_5 = 0.70$). With this constraint and the constraint of overall pentablock symmetry ($f_1 = f_5$, $f_2 = f_4$), the parameter space for our SCFT model of a pentablock melt is effectively two-dimensional: one composition variable, f_3 (an arbitrary choice) and one interaction strength, $h = \chi_{\mathrm{AB}} N$. We further eliminate h from consideration by fixing it at a value, $h = 45$, sufficient to produce microphase separation in the melt. (Increasing h will generally have the effect of improving solid-state mechanical performance while diminishing the melt processability of the material, so a compromise is generally struck in specific applications.) This leaves only the midblock composition variable f_3 to be varied in the search for optimal practical toughness.

As indicated in section I, our strategy is to identify molecular designs that maximize the fraction of center A blocks that bridge between neighboring B-rich microdomains. Our calculations are relevant for equilibrated pentablock melts that are above the glass transition temperatures of both A and B blocks; we assume that the bridge-loop statistics do not change appreciably as the materials are cooled to the solid state at use temperature. Further, we utilize the experimental observations of Ryu, Hermel, and co-workers[15,16,18] to associate increases in the number of bridging chains within the continuous A phase with improvements in solid-state toughness (cf. Figure 1). Again we note that morphological (e.g., grain size) and processing factors clearly also impact practical toughness, so we assume that such factors are held fixed during our investigation. With these caveats, we embark on a study of the fraction of center A blocks in bridged conformations, f_{br}, upon varying the center block fraction f_3. More specifically, we consider a symmetric ABABA pentablock melt at $h = 45$ and evaluate f_{br} over the range $0.12 \leq f_3 \leq 0.54$, in which the equilibrium morphology is a hexagonal array of B-rich cylinders in a continuous A matrix.

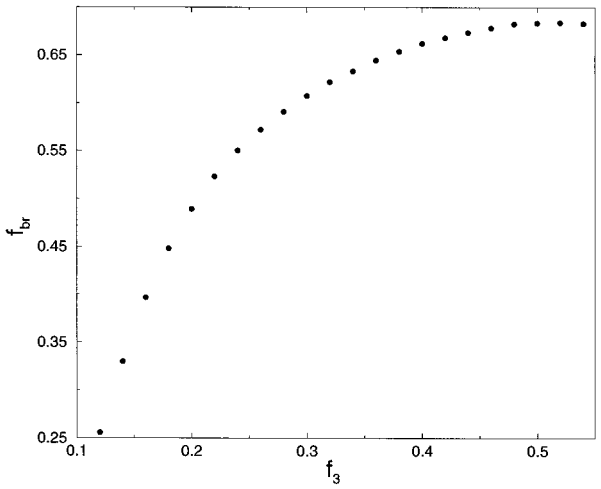

Figure 5. Average fraction of middle A blocks (block 3) that bridge between B cylinders as a function of the midblock length f_3 for symmetric ABABA pentablock copolymers. The overall A volume fraction was fixed at $f_A = f_1 + f_3 + f_5 = 0.7$ as f_3 was varied in these calculations. The interaction strength was $h = 45$.

To obtain the bridging fraction at a fixed value of f_3, we first solved the SCF equations on a two-dimensional grid with lattice spacing $\Delta x = 0.1 R_{\mathrm{g}}$, where $R_{\mathrm{g}}^2 = Nb^2/6$ is the unperturbed mean-squared radius of gyration of a pentablock copolymer. The free energy of the "equilibrium" structure obtained from that first calculation was then minimized with respect to the size of the simulation cell. The diffusion equation for q was solved using 101 "contour" steps, and we have verified that the results obtained are insensitive to an increase in that number. The calculations for the range of f_3 were performed in parallel using the Beowulf cluster of Linux PCs in the UCSB-MRSEC Central Computing Facility.

A typical composition pattern, i.e., the total A density field $\phi_{\mathrm{A}}(\mathbf{r})$, is shown in Figure 3 for $f_3 = 0.52$. The corresponding Voronoi diagram for this pattern is shown in Figure 4 and was used to establish a center A block bridge fraction of $f_{\mathrm{br}} = 0.68$. Repeating such calculations over $0.12 \leq f_3 \leq 0.54$ leads to the variation of f_{br} with f_3 shown in Figure 5. We note a rapid rise in the bridge fraction as f_3 is increased to 0.2, a slower rise over the interval $0.2 \leq f_3 \leq 0.4$, and a saturation of f_{br} to a plateau value of about 0.68 as f_3 is increased beyond 0.4. Associating bridge fraction with toughness, it is evident from the figure that toughness should be optimal (within the cylindrical morphology) when f_3 is adjusted to a value in the vicinity of 0.5. Higher values of f_3 will ultimately reduce strength through pull-out of the dangling A ends, so the maximum in practical toughness will likely be achieved at the low end of the saturation range of f_{br}. In summary, we anticipate that symmetric ABABA pentablocks with a 70% overall glass content should be optimally tough when there is roughly a five-to-one ratio of central to end A block lengths, $f_3/f_1 \approx 5$, i.e., a 10−15−50−15−10 structure in volume percentages of the five blocks. This conclusion likely has a weak dependence on the specific values of $f_{\mathrm{A}} = 0.7$ and $h = 45$ that were selected but nevertheless should prove useful.

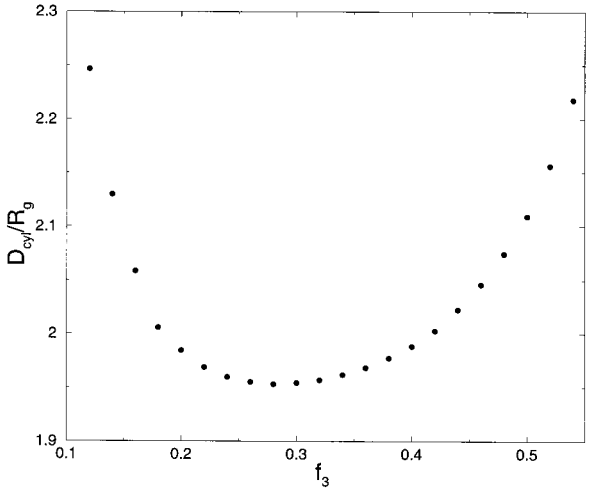

Figure 6. Average distance between neighboring cylindrical B-rich domains for the same series of symmetric pentablocks considered in Figure 5. In the case of short midblock lengths, $f_3 \leq 0.2$, the intercylinder spacing is evidently controlled by the longer outer A blocks and drops rapidly as their size is decreased (f_3 is increased). Conversely, for long midblocks, $f_3 \geq 0.4$, the intercylinder spacing is controlled by the center A block length and rises with increasing f_3. In the intermediate composition range, there is little variation of the domain spacing with f_3. The bridging fraction of the central A block (Figure 5) rises most rapidly with f_3 when the terminal A blocks control the domain spacing.

We can gain some physical insight into the bridge fraction trend observed in Figure 5 by examining the average spacing between the centers of adjacent B-rich cylinders, D_{cyl}, for the same range of f_3. As shown in Figure 6, there is a rapid drop in the intercylinder spacing over the interval $0.12 \leq f_3 \leq 0.20$, which mirrors the rapid rise in f_{br} over the same interval. Evidently, for such cases of short central A blocks, the intercylinder spacing is controlled by the length of the outer A blocks. Increasing f_3 shrinks the outer A blocks 1 and 5 according to $f_1 = f_5 = (0.7 - f_3)/2$, which in turn decreases D_{cyl}. This contraction of D_{cyl} also makes it possible for larger numbers of central A blocks to bridge between neighboring cylinders. Over the interval $0.4 \leq f_3 \leq 0.54$, Figure 6 shows a rapid rise of D_{cyl} with f_3. In this regime, where the center A blocks are the longest, the intercylinder spacing is evidently controlled by their length. Raising f_3 increases the length of the center blocks, which permits the B-rich cylinders to move farther apart. The growth in f_{br} is apparently saturated in this regime because although the midblocks are longer and are thus more able to bridge, the distance D_{cyl} over which they must span is continuously increasing with f_3—hence favoring loops.

Further insight into the bridging and looping phenomena can be gained by examining different components of the block density fields. For example, Figure 7 shows the density pattern of the terminal A block (1 or 5) for the configuration shown in Figure 3. The light regions correspond to high densities of terminal A blocks (1 or 5), while dark regions correspond to low densities of the same blocks. Comparison of Figures 3 and 7 indicates that the short terminal A blocks ($f_1 = f_5 = 0.09$) are strongly localized at the outer surface of the B-rich cylinders. These short A blocks also penetrate a substantial distance inside the cylinders, effectively broadening the A−B interfaces. Evidently, the long central A blocks fill in the gaps between cylinders, with nearly 70% of these blocks residing in bridged conformations.

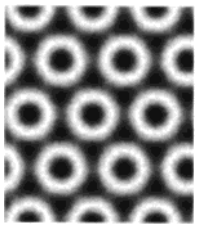

Figure 7. Density field $\phi_A^1(\mathbf{r})$ of the terminal A block 1 (and by symmetry block 5) for a symmetric pentablock with the same parameters as Figure 3: $f_1 = f_5 = 0.09$, $f_2 = f_4 = 0.15$, $f_3 = 0.52$, and $h = \chi_{AB}N = 45$. Under these conditions, the short terminal A blocks (light regions) are strongly localized to the outer surfaces of the B-rich cylinders and contribute a substantial broadening of the AB interfaces.

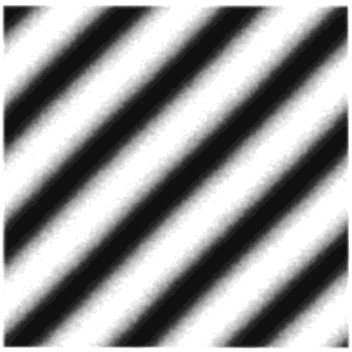

Figure 8. Morphological transition to a lamellar phase induced by a 3 to 1 ratio of outer to inner A block lengths in a symmetric pentablock copolymer melt. The total A density field $\phi_A(\mathbf{r})$ is shown (B is dark) for a melt with parameters $f_1 = f_5 = 0.30$, $f_2 = f_4 = 0.15$, $f_3 = 0.10$, and $h = 45$. Note that the overall volume fraction of A is the same as in Figure 3, $f_A = 0.70$.

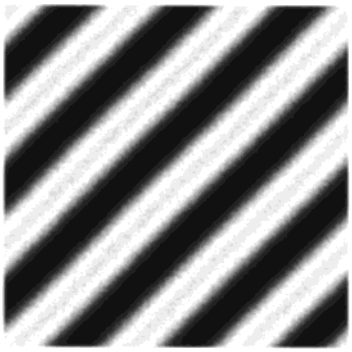

Figure 9. Center A block density field, $\phi_A^3(\mathbf{r})$, for the same pentablock copolymer mesophase as in Figure 8 (dark corresponds to lowest density of block 3). The short central A blocks are evidently mixed into the B-rich domains as well as strongly localized on their surfaces.

Outside of the composition range $0.12 \leq f_3 \leq 0.54$, transitions to other mesophase structures are possible. For example, Figure 8 shows the total A monomer density field for a lamellar phase that is lower in free energy than the hexagonal phase for $f_3 = 0.10$, $f_A = 0.7$, and $h = 45$. This situation corresponds to a three-to-one ratio of outer to inner A block lengths, $f_1/f_3 = 3$. Insight into the morphological transition to lamellae can be gained by examining the density field for the short center A block, $\phi_A^3(\mathbf{r})$. In Figure 9 we show this field, again with light corresponding to high density and dark to low density. Comparison of Figures 8 and 9 indicates

that the short central A blocks are nearly completely mixed into the B-rich layers. For the purpose of explaining the phase behavior of these pentablocks, we can thus think of each molecule as an *effective triblock*, where blocks 2, 3, and 4 are lumped into a single C block of composition $f_C = f_2 + f_3 + f_4 = 0.4$. For this effective ACA triblock copolymer with $f_C = 0.4$, the lamellar phase is expected to have a lower free energy than the hexagonal phase,[22] in agreement with our result. We also observe a transition to a lamellar structure when f_3 is increased above 0.54. In that case, the small A end blocks mix uniformly inside the B-rich lamellae, and we can envision the pentablock as an effective CAC triblock. Because the limiting architecure at $f_3 = 0.7$ is a BAB triblock with $f_A = 0.7$, a second transition to a cylindrical morphology occurs as the length of the middle block is further increased. We note that our two-dimensional calculations rule out the possibility of intrinsically three-dimensional structures, such as the gyroid phase, which may be stable for a small range of f_3 values.

From the standpoint of toughness, it has been observed[24] that lamellar phases are more ductile and tough than hexagonal phases for both PCHE−PE−PCHE and PCHE−PE−PCHE−PE−PCHE architectures. Presumably this is a manifestation of the geometrical cylinder to sheet transition of the soft (and entangled) PE phase that occurs when a hexagonal phase is transformed to a lamellar phase. Thus, symmetric ABABA pentablocks with $f_A = 0.7$ might exhibit a *toughness discontinuity* on varying f_3 over the range of $0.10 \leq f_3 \leq 0.12$. A rather "weak" hexagonal phase with $f_{br} \approx 0.33$ at $f_3 = 0.12$ could transform into a significantly tougher lamellar phase as f_3 is decreased toward 0.10.

4. Application to Complex Block Copolymer Phases

As mentioned previously, the methodology of section II is equally applicable to more complex block copolymers, such as the ABC systems that have garnered a lot of recent experimental attention. In the present section, we provide a few examples of Voronoi lattice construction and bridge fraction calculations for some interesting mesophases that were obtained recently using SCFT for linear ABCA tetrablock copolymers. In thermoplastic elastomer applications, one might envision a realization of such materials where the A blocks are hard and glassy, while both the B and C blocks are soft and elastomeric at the use temperature—yet are immiscible with each other. The morphologies shown in Figures 10 and 11 were obtained with equal-volume A blocks and with all three binary interaction strengths (h_{AB}, h_{BC}, h_{AC}) set to 35. At composition $f_A = 0.26$ and $f_{BC} = 0.37$ (Figure 10), the melt microphase separates into B-rich and C-rich lamellae with small A decorations located at regular intervals along the interfaces. Instead, at nearly equal volume fraction of the three species ($f_A = 0.34$ and $f_{BC} = 0.33$, Figure 11), the copolymer chains self-assemble into a three-color hexagonal phase. The Voronoi lattice constructed around the A-rich aggregates is shown for both patterns. To calculate the fraction of chains that have their middle B and C blocks bridging different A-rich domains, we proceed as for the pentablock copolymers. In this case, however, the function $\bar{q}$ (see eq 8) is first defined at $s = f_A/2$ and then propagated along the chain contour to $s = f_A/2 + f_B + f_C$. For the mesophase configurations

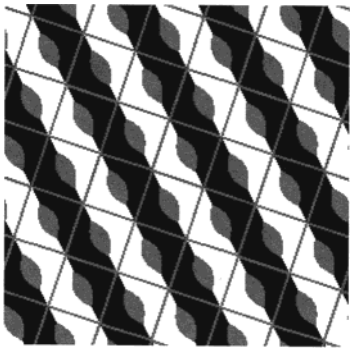

Figure 10. Mesophase obtained by solving the SCF equations for a melt of ABCA tetrablock chains of composition $f_A = 0.26$ and $f_{B,C} = 0.37$. Regions rich in A, B, or C monomers are shown in gray, black, and white, respectively. A Voronoi diagram constructed around the A-rich aggregates is also shown.

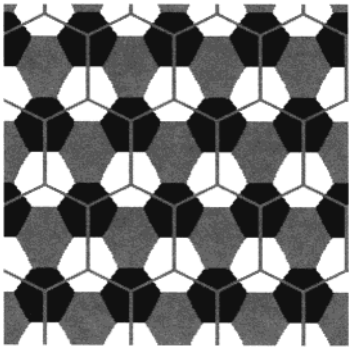

Figure 11. Mesophase obtained by solving the SCF equations for a melt of ABCA tetrablock chains of composition $f_A = 0.34$ and $f_{B,C} = 0.33$. Regions rich in A, B, or C monomers are shown in gray, black, and white, respectively. A Voronoi diagram constructed around the A-rich aggregates is also shown.

shown in Figures 10 and 11, the calculation yields the bridge fractions $f_{br} = 0.60$ and $f_{br} = 0.56$, respectively. Presumably calculations of this sort could be used to assist the screening of candidate ABCA mesophases for their mechanical performance as thermoplastic elastomers.

5. Summary and Discussion

In the present paper we have shown how the computational approach pioneered by Matsen and Schick for studying bridging and looping in block copolymers can be adapted to analyze mesophases computed using a real-space, "discovery engine" implementation of SCFT. To the extent that the fraction of internal blocks exhibiting bridged conformations can be associated with one or more physical properties, this adaptation constitutes a "property engine" that can be used for computational−combinatorial exploration of molecular designs that optimize the property set. In section III, we provided a specific example of this approach to the problem of toughness optimization in symmetric ABABA pentablock copolymers, where A is a rigid/glassy species in the majority ($f_A = 0.7$) and B is a minority soft/elastomeric component. Such materials could be designed to serve as tough−rigid−clear thermoplastics. Using experimental evidence for a relationship between the fraction of center A blocks that bridge B microdomains and practical toughness, we were able to apply the above tools to argue that 10−15−50−15−10 (block compositions in volume percent) pentablock copolymers

should be optimally tough within a family of copolymers consistent with a 70% glass content (for high modulus). We await experimental tests of this prediction.

In section IV, we argued that the same methodology can be applied to the complex mesophases that are characteristic of three-color ABC and ABCA block copolymers. In such systems, the possibilities for self-assembly are almost unlimited, and the parameter spaces for elucidating mesophase structures are extremely large. Thus, an automated, parallel approach to sorting computed structures according to some physical property would be highly desirable. In some cases, it may turn out that the simple bridge fraction property engine outlined here is sufficent to rank order some useful property, such as toughness, among the various mesophases. In other situations, one may need to build a more sophisticated property engine that reads in the equilibrated density patterns from the SCFT discovery engine and applies a code, e.g., a finite element composite medium code,[25] for physical property estimation. With an efficient implementation of one or more such property engines, it should be possible to carry out massively parallel screenings of copolymer designs to optimize desired property sets.

We end by commenting that the general computational strategy outlined here is more broadly applicable to the design of polymer alloys (two- and three-phase plastics containing block or graft copolymers) and solution-borne formulations (shampoos, cremes, copolymer gels, personal care products, etc.), as opposed to the pure block copolymer systems examined in the present paper. Integrated numerical design tools could serve to greatly accelerate experimental development efforts in these areas and potentially lead to entirely new avenues for product design.

Acknowledgment. This work was partially supported by the MRSEC Program of the National Science Foundation under Award DMR-96−32716. Extensive use was made of the UCSB-MRSEC Central Computing Facilities. Acknowledgment is also made to the donors of the Petroleum Research Fund, administered by the ACS, and the Dow Chemical Company for partial support of this research. The authors are grateful to C. Y. Ryu, E. J. Kramer, C. Leibig, and S. F. Hahn for helpful discussions.

References and Notes

(1) Bates, F. S.; Fredrickson, G. H. *Phys. Today* **1999**, *52*, 32.
(2) Hamley, I. W. *The Physics of Block Copolymers*; Oxford University Press: Oxford, 1998.
(3) Matsen, M. W.; Bates, F. S. *Macromolecules* **1996**, *29*, 1091.
(4) Matsen, M. W.; Schick, M. *Phys. Rev. Lett.* **1994**, *72*, 2660.
(5) Matsen, M. W.; Schick, M. *Curr. Opin. Colloid Interface Sci.* **1996**, *1*, 329.
(6) Auschra, C.; Stadler, R. *Macromolecules* **1993**, *26*, 2171. Breiner, U.; Krappe, U.; Thomas, E. L.; Stadler, R. *Macromolecules* **1998**, *31*, 135.
(7) Brinkmann, S.; Stadler, R.; Thomas, E. L. *Macromolecules* **1998**, *31*, 6566. Goldacker, T.; Abetz, V. *Macromolecules* **1999**, *32*, 5165.
(8) Shefelbine, T. A.; Vigild, M. E.; Matsen, M. W.; Hajduk, D. A.; Hillmyer, M. A.; Cussler, E. L.; Bates, F. S. *J. Am. Chem. Soc.* **1999**, *121*, 8457.
(9) Mogi, Y.; Kotsuji, H.; Kaneko, Y.; Mori, K.; Matsushita, Y.; Noda, I. *Macromolecules* **1992**, *25*, 5408. Matsushita, Y.; Suzuki, J.; Seki, M. *Physica B* **1998**, *248*, 238.
(10) Sioula, S.; Hadjichristidis, N.; Thomas, E. L. *Macromolecules* **1998**, *31*, 5272, 8429.
(11) Drolet, F.; Fredrickson, G. H. *Phys. Rev. Lett.* **1999**, *83*, 4317.
(12) Bohbot-Raviv, Y.; Wang, Z.-G. *Phys. Rev. Lett.* **2000**, *85*, 3428.
(13) Fraaije, J. G. E. M.; van Vlimmeren, B. A. C.; Maurits, N. M.; Postma, M.; Evers, O. A.; Hoffmann, C.; Altevogt, P.; GoldbeckWood, G. *J. Chem. Phys.* **1997**, *106*, 4260. van Vlimmeren, B. A. C.; Maurits, N. M.; Zvelindovsky, A. V.; Sevink, G. J. A.; Fraaije, J. G. E. M. *Macromolecules* **1999**, *32*, 646.
(14) Dotera, T. *Phys. Rev. Lett.* **1999**, *82*, 105. Dotera, T.; Hatano, A. *J. Chem. Phys.* **1996**, *105*, 8413.
(15) Ryu, C.-Y.; Fredrickson, G. H.; Hahn, S. F.; Kramer, E. J. *Proc. of 11th Intern. Conf. on Deformation, Yield, and Fracture of Polymers*; The Inst. of Materials: London, 2000; pp 80−87.
(16) Hermel, T., unpublished data.
(17) The acronym PCHE refers to the alternate name for this polymer−poly(cyclohexylethylene).
(18) Ryu, C.-Y., unpublished data.
(19) Leibig, C., unpublished data.
(20) Matsen, M. W.; Schick, M. *Macromolecules* **1994**, *27*, 187.
(21) Matsen, M. W. *J. Chem. Phys.* **1995**, *102*, 3884.
(22) Matsen, M. W.; Thompson, R. B. *J. Chem. Phys.* **1999**, *111*, 7139.
(23) Matsen, M. W. *Curr. Opin. Colloid Interface Sci.* **1998**, *3*, 40.
(24) Weiman, P. Doctoral Dissertation, University of Minnesota, 1998.
(25) Gusev, A. A. *J. Mech. Phys. Solids* **1997**, *45*, 1449.

MA0100753